

Research Article

Development of the Large-Tonnage Pressure-Type Prestressed Anchor Cable with BFRP for Geotechnical Engineering and Its Mechanical Properties

Zhigang Du ^{1,2}, Ning Li ¹, Wuxiu Ding ¹, Yawen Tao,^{1,3} Xiaolei Wu,¹ Jinjun Guo,¹ Peng You,⁴ Chaoqin Wang,⁴ Paul Archbold,⁵ Brian Mullarney,⁵ and Bing Xie¹

¹School of Civil Engineering, Luoyang Institute of Science and Technology, Luoyang 471023, China

²Yima Coal Corporation, Henan Energy Group Corporation, Sanmenxia 472000, China

³College of Civil Engineering and Architecture, Henan University of Technology, Zhengzhou 450000, China

⁴Center of Highway Development, Luoyang 471023, China

⁵School of Engineering & Materials Research Institute, Athlone Institute of Technology, Westmeath N37 HD68, Ireland

Correspondence should be addressed to Ning Li; wuzhilining@126.com

Received 22 July 2022; Accepted 22 August 2022; Published 13 September 2022

Academic Editor: Su Shan-Jie

Copyright © 2022 Zhigang Du et al. This is an open access article distributed under the Creative Commons Attribution License, which permits unrestricted use, distribution, and reproduction in any medium, provided the original work is properly cited.

Prestressed anchor cable is widely used in geotechnical engineering to control the displacement or landslide of an unstable slope. However, the traditional cable anchor is made of steel material, which is easy to get rust in a corrosive environment. Basalt fiber-reinforced plastics (BFRP) are a kind of emerging compound material, with a good performance of high strength, low weight, and anticorrosion. Herein, an innovative large-tonnage pressure-type prestressed anchor is made with BFRP. This large-tonnage BFRP anchor cable has seven bunch structures of the “BFRP-connector-strand.” In each bunch of the “BFRP-connector-strand,” three BFRP tendons and one steel strand are connected inside a steel sleeve connector using the epoxy resin adhesive. The ultimate load-bearing capacity of this BFRP cable anchor can reach 202.38 tonnages. At the ultimate tensioning force condition, the strain of BFRP tendons for this large-tonnage BFRP anchor cable ranges from 1.51% to 1.76%. In the tensioning operation, there is a linear growth relationship between the tensioning force and the strain for this BFRP cable anchor. Once the tensioning force reaches the ultimate strength of this BFRP anchor cable, this cable will present system failure. This situation primarily results from the failure of the “BFRP-connector-strand.” The failure modes of this BFRP anchor cable can be classified into three types: the steel strand rupture, the steel connector rupture, and the BFRP tendon rupture. During the tensioning operation, due to the length difference of the BFRP tendons, this large-tonnage BFRP cable anchor presents an end-off-axis effect. It makes the load bearing of the BFRP tendons 5.00–6.60 times larger than that of the no end-off-axis effect. Nevertheless, due to the plastic deformation of the end steel anchor sleeve, the influence of the end-off-axis effect decreases with the increase of applied tensioning force. The load-bearing capacity of this large-tonnage BFRP cable anchor reaches 87.70–91.50% of its theoretical value.

1. Introduction

Prestressed anchor cable is widely used in the slope treatment of bridges, high-speed railways, tunnels, reservoirs, underground space engineering, and so on [1–5]. However, the traditional anchor cable is made of steel material, which is easy to get rust in a watery environment [6–10]. Once the steel material gets rusts, the carried prestress by the anchor

cable will significantly decrease, which can cause the failure of the anchoring engineering. Besides, the steel material has a high density, which is cumbersome and physically consumed for its application in the mountain and ravine regions.

In contrast with the steel material, BFRP is a kind of new composite material, with a performance of improved elastic modulus, high strength, lightweight, good corrosion

resistance, excellent stability to temperature, and low cost [11–13]. Many scholars have attempted to use the BFRP instead of the steel material to develop the prestressed anchor cable in the geotechnical anchoring engineering field [14–17]. However, because of its anisotropic property, the shear strength of the BFRP is much lower than its tensile strength. The most efficient way to use BFRP is to apply it as a tension element. In the development of the BFRP anchor cable, due to the stress concentration, the BFRP tendon often has a shear failure at the tensioning end without difficulty [18, 19]. At that time, the load-bearing capacity of the BFRP tendon is far less than its ultimate tensile strength. The lower transversal shear strength of the BFRP tendon dramatically limits its application. Several approaches to changing the BFRP tendon's structure have been proposed to resolve this problem. For instance, one specific improvement measure is strengthening the tensioning end of the BFRP tendon with a bonded steel sleeve [14, 17, 20]. By this treatment, the tensioning equipment's applied force will directly act on the steel sleeve instead of the BFRP tendon. Then, the tensioning force is completely transferred by the bond stress along with the two interfaces, the interface of the BFRP tendon and the adhesive, and the interface of the steel sleeve and the adhesive. This type of bonding anchor is most commonly used for the small-diameter BFRP tendon, and its load-bearing capacity is low.

However, with the development of major geotechnical anchoring engineering, the requirement for the load-bearing capacity of the prestressed anchor cable is always growing. For instance, in the sizeable hydraulic project of the China Three Gorges Dam, more than 3975 prestressed steel strand anchor cables with a load-bearing capacity of 300.00 tonnages are adopted [21]. Though some BFRP anchor cables have been developed, most of them have a load-bearing capacity of fewer than 100.00 tonnages. The load-bearing capacity of these BFRP anchor cables is far less than the need for significant geotechnical anchoring engineering. Therefore, this study is aimed at developing a large-tonnage BFRP anchor cable and discussing its mechanical properties.

2. Materials and Methods

2.1. Materials. For geotechnical anchoring engineering, there are two types of prestressed anchor cables: the tension-type prestressed anchor cable and the pressure-type prestressed anchor cable. In mechanics, compared to the tension-type prestressed anchor cable, the pressure-type prestressed anchor cable transfers the applied prestress to the load-bearing plate at the end of the anchor cable and makes it act on the anchorage body in the way of pressure force. Due to the higher-pressure resistance of the anchorage body, the pressure-type prestressed anchor cable is widely used for geotechnical anchoring engineering. The materials used in this study to develop this large-tonnage pressure-type BFRP anchor cable include the BFRP tendon, steel strand, steel sleeve, epoxy resin adhesive, and circle load-bearing plate. The material properties and parameters are listed in Table 1.






2.2. Structure Design of the Large-Tonnage Pressure-Type Prestressed BFRP Anchor Cable. As a typical transverse anisotropic material, the shear strength of the BFRP tendon is much lower than its tensile strength. During the development of the BFRP anchor cable, it shows that as the tensioning equipment directly acts on the BFRP tendon, the stress concentration between the steel wedge and the BFRP tendon often causes the shear failure of the BFRP. In this situation, the load-bearing level of the BFRP tendon is far less than its ultimate strength. To avoid this issue and maximize its load-bearing level, it was innovatively proposed to adopt a middle connector to connect the BFRP tendon and the steel strand. Then, make the steel strand, instead of the BFRP tendon, to be used as the tensioning end. Besides, considering the engineering geology condition of the China Three Gorges reservoir area, a large-tonnage BFRP anchor cable (prestress more than 100.00 tonnages) needs to be developed to strengthen the slope of the unstable rock slope.

The materials used to develop this large-tonnage pressure-type BFRP anchor cable are listed in Table 1. This developed large-tonnage pressure-type BFRP anchor cable includes two subsystems: one is the cable rope structure system and the other is the end structure system. For the cable rope structure system, several procedures are followed. First, the cable rope structure subsystem, termed as the “BFRP-connector-strand,” is made, where a steel strand and three BFRP tendons were butting connected inside the steel sleeve connector by injecting the epoxy resin adhesive (Figures 1(a)–1(d)). Then, the end structure system is made. The end structure system includes a circle load-bearing plate and an end anchor sleeve. When the “BFRP-connector-strand” is made in the first step, make the BFRP end of the “BFRP-connector-strand” pass through the holes of the circle load-bearing plate and fix it in the end anchor sleeve with epoxy resin adhesive. For the end structure system, the end anchor sleeve can be just sited in the hole month of the circle end load-bearing plate (Figure 1(e)).

By those processes, this pressure-type large-tonnage prestressed anchor with one bunch of the “BFRP-connector-strand” is made (Figure 2). As the prestress was applied at the tensioning end of the steel strand, it will transfer and act on the circle load-bearing plate in the form of compression force.

2.3. Structure Optimization of the Large-Tonnage Pressure-Type BFRP Anchor Cable. In developing the large-tonnage pressure-type BFRP anchor cable, four types of steel strands were used to make the “BFRP-connector-strand.” The strength of each of the “BFRP-connector-strand” is listed in Table 2. The strength test shows that the steel strand structure in the steel sleeve connector influences the load-bearing capacity of the BFRP anchor cable significantly. The load-bearing capacity of the “BFRP-connector-strand” for the normal steel strand is 146.00 kN. When the steel strand was treated as a quartz sand-coated steel strand, sputtering-treated steel strand, and surface-indented steel strand, the load-bearing capacities of the “BFRP-connector-strand” were 165.92 kN, 185.66 kN, and 336.97 kN, respectively. With the increase of the bonding

TABLE 1: The material properties and parameters for developing the large-tonnage BFRP anchor cable.

| Materials | Descriptions | Illustration |
|---------------------------|--|---|
| BFRP tendon | The BFRP tendon is made by Shanxi ECIC Basalt Development Co. Ltd., China. Its diameter is 12.60 mm and is quartz sand surface coated. The size of the quartz sand is 20.00 to 40.00 mesh. The tensile strength and elastic modulus of the BFRP tendon are 891.00 MPa and 48.45 GPa, respectively. |  |
| Steel strand | The specification of the steel strand is 1 × 7–21.60 mm, which meets the Chinese National Standard [22]. Its tensile strength is 1860.00 MPa, the maximum load-bearing capacity is 58.70 tonnage, and the ultimate elongation is 3.50%. |  |
| Steel sleeve | It is made of 40 Cr steel, whose inner diameter is 32.00 mm and outer diameter is 38.50 mm. The inner wall of the steel sleeve is covered with thread 0.50 × 0.50 mm. When it is used as the middle connector, one component of the developed BFRP anchor cable herein, its length is 80.00 cm. When it is used as the end anchor sleeve, another element of the designed BFRP anchor cable, its length is 40.00 cm. |  |
| Epoxy resin adhesive | It is a two-part epoxy (MKT – GSS/L), which is produced by Nanjing Mankat Technology Co. Ltd., China. Its compressive strength is 72.40 MPa, tensile strength is 46.20 MPa, flexural strength is 70.80 MPa, shear strength is 21.40 MPa, the elastic modulus is 3.10 GPa, and the maximum elongation is 1.50%. It was used as the adhesive filler to fix the BFRP tendon and the steel strand inside the sleeve. |  |
| Circle load-bearing plate | This circle load-bearing plate was a component of the developed BFRP anchor cable herein, which was made of 40 Cr steel. It is cylindrical with seven holes; its diameter and height are 149.00 mm and 50.00 mm, respectively. Each of the holes is T shaped, whose month diameter is 39.00 mm with a height of 5 mm and whose body diameter is 31.00 mm with a height of 45.00 mm. |  |

force between the surface-indentated steel strand and the epoxy resin adhesive, the load-bearing capacity of the BFRP anchor cable increases significantly.

The failure mode of the “BFRP-connector-strand” for the normal steel strand, the quartz sand-coated steel strand, and the sputtering-treated steel strand is the steel strand pulled out from the connector, where the BFRP tendon is complete. It indicates that the load-bearing capacity of the BFRP tendon has not reached its tensile strength in those situations. However, for the surface-indentated steel strand, the failure mode of the “BFRP-connector-strand” is the BFRP tendon rupture. It indicates that the bonding stress completely transfers the tensioning force along with the interfaces of the BFRP tendon and the adhesive and the steel sleeve and the adhesive interface. Thus, the surface-indentated steel strand was adopted for making the “BFRP-connector-strand.”

Based on the above results, the large-tonnage pressure-type BFRP anchor cable with seven bunches of “BFRP-connector-strand” was developed (Figure 4).

2.4. *Methods for the Mechanical Property Measurement of the Large-Tonnage Pressure-Type BFRP Anchor Cable.* To achieve the load-bearing capacity of this developed BFRP anchor cable, the strength test was employed according to the following sequence of first single bunch tensioning and then system tensioning (Figure 5). The applied tensioning force of this pressure-type anchor cable will compress the reaction frame of the tensioning system by the circle load-bearing plate. In these two-tensioning processes, the front clamp jack with a 450.00 kN measure range (YCQ45Q-200 type made by China) and the center hole jack with a 3000.00 kN measure range (YCQ300Q-200A type made by China) were taken. The tensioning force was applied

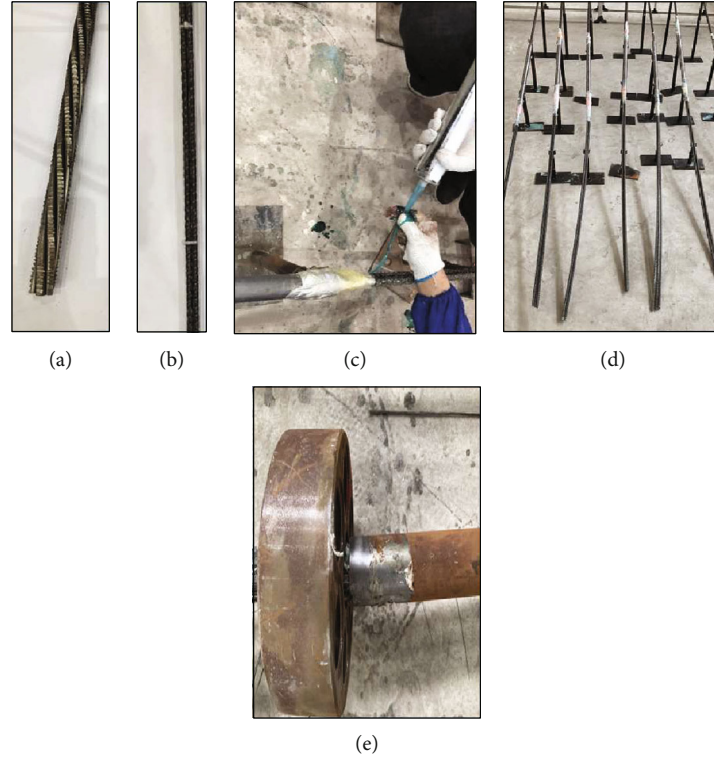


FIGURE 1: The procedure for making the BFRP anchor cable: (a) the steel strand, (b) the BFRP tendon, (c) injecting epoxy resin adhesive, (d) the “BFRP-connector-strand” illustration, and (e) the end structure.

according to the Chinese National Standard [23]. Besides, in the strength test process, the elongation value of the BFRP anchor cable was measured by the linear displacement sensor, which was made by Jiangsu Donghua Measurement Technology Co. Ltd., China. Its accuracy is 0.01% mm. The strain of the BFRP tendons in the process of tensioning operation was measured by the electric resistance strain gauge. Its accuracy is $10^{-6}\epsilon$, and the data collection frequency is 5.00 Hz.

In the single bunch tensioning test of this large-tonnage BFRP anchor cable, the tensioning operation was carried out in the sequence of *G*, *A*, *D*, *F*, *C*, *E*, and *B* for the sake of tensioning convenience. As the tensioning force for each bunch reaches 55.00% of its ultimate strength, the system tensioning was taken to achieve the ultimate strength of this large-tonnage BFRP anchor cable (Figure 6). In the stage of single bunch tensioning, the tensioning force was gradually applied by a level of 5.00% of its ultimate strength. In the stage of the system tensioning, the tensioning force was also gradually applied by a level of 2.50% of its ultimate strength. The ultimate theoretical strength for this large-tonnage BFRP anchor cable can be achieved by the following:

$$f_{ptk} = f_i \cdot X, \quad (1)$$

where f_i is the ultimate strength of each “BFRP-connector-strand,” 336.97 kN, signed by f_{ptk-1} ; X is the number of the “BFRP-connector-strand.” Thus, according to equation (1), it was achieved that the ultimate theoretical strength of this

large-tonnage BFRP anchor cable can be 2358.80 kN, signed by f_{ptk-2} .

3. Results and Discussions

3.1. The Mechanical Performance of the Developed BFRP Anchor Cable during the Stage of Single Bunch Tensioning. Figure 7 shows the relationship between the deformation and the tensioning force for this BFRP anchor cable in the process of single bunch tensioning. For the same tensioning force, there is a slight difference in the elongation value for each bunch of the “BFRP-connector-strand.” As the applied tensioning force reaches $0.55f_{ptk-1}$ (i.e., 183.15 kN), the elongation values of the *A*, *B*, *C*, *D*, *E*, *F*, and *G* bunches of the “BFRP-connector-strand” were 2.37, 2.01, 1.80, 1.96, 1.91, 2.16, 2.17, and 2.05 mm. This difference in elongation value can be clarified and explained by the following reasons. Firstly, there are gaps between the interval reaction frame for tensioning. Though a prestress of $0.1f_{ptk-1}$ is applied to the BFRP anchor cable before the experiment procedure starts, it is not enough to remove these gaps. As the tensioning experiment was performed according to the designed scheme, these gaps will be compressed again and again by the multiapplied tensioning force during the process of the single bunch tensioning. These changing gaps between the interval reaction frame make the elongation value different for each bunch of the “BFRP-connector-strand.” Besides, the system error during the tensioning operation and the manually manufacturing the BFRP anchor cable can also

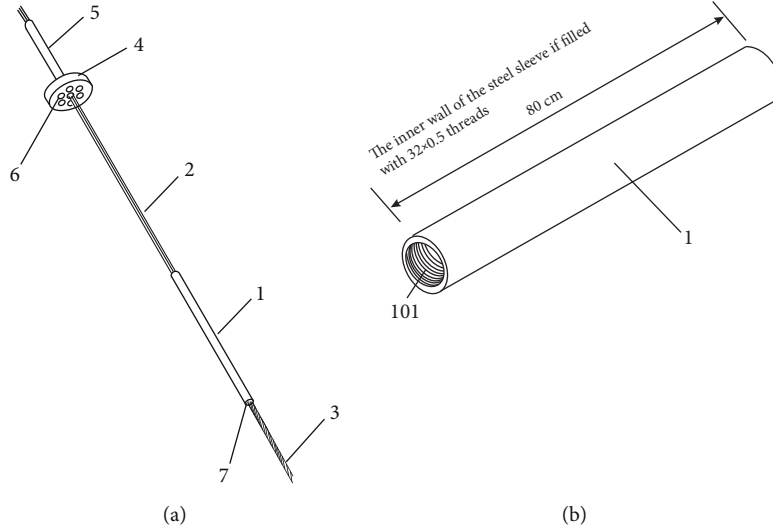


FIGURE 2: The illustration of the pressure-type BFRP anchor cable: (a) the single bunch of the large-tonnage BFRP anchor cable and (b) the inner wall of the steel sleeve filled with threads.

TABLE 2: Strength test of the “BFRP-connector-strand.”

| Steel strand structure for the “BFRP-connector-strand” | Strength of the “BFRP-connector-strand” | The failure mode of the “BFRP-connector-strand” |
|--|---|--|
| Normal steel strand | 146.00 kN | Steel strand pulled out from the connector (Figure 3(a)) |
| Quartz sand-coated steel strand | 165.92 kN | Steel strand pulled out from the connector |
| Sputtering-treated steel strand | 185.66 kN | Steel strand pulled out from the connector |
| Surface-indentated steel strand | 336.97 kN | BFRP tendon rupture (Figure 3(b)) |

result in a difference in the elongation value. No matter what, it can be seen that, for this BFRP anchor cable, there is a good linear relationship between the elongation value and the applied tensioning force.

Figure 8 shows the relationship between the strain and the tensioning force for this BFRP anchor cable. The signs, such as A-J-1, A-J-2, and A-J-3, represent the strain of the three BFRP tendons in the A bunch of the “BFRP-connector-strand.” Identical meanings are attached to B-J-1, B-J-2, B-J-3, and so on. Of which, the strains signed by D-J-3 and E-J-3 were not collected for the strain gauge being destroyed in the tensioning of the D bunch and the E bunch. So, there is a lack of those data.

It can be seen that there is also a difference in the strain for each of the BFRP tendons. During the stage of single bunch tensioning, the applied tensioning force is shared not only by the BFRP tendons but also by the friction between the bunches of the “BFRP-connector-strand.” Besides, as before mentioned, the gaps among the interval reaction frame are compressed again and again by the multi-applied tensioning force. This behavior of the continuously compressed gap by the later tensioning operation creates a stress relaxation effect for the former tensioned BFRP tendons. Therefore, by these factors, the difference in the strain of the BFRP tendons exists. To analyze the load-bearing level of the BFRP tendons in the process of tensioning operation, the load shared by this large-tonnage BFRP anchor cable is

achieved by the followings

$$f_i = 3 \cdot \epsilon_i \cdot E \cdot S (i = A, B, C, D, E, F, G),$$

$$f_t = \sum_i f_i (i = A, B, C, D, E, F, G), \quad (2)$$

where f_t is the load-bearing level by this large-tonnage BFRP anchor cable in the process of tensioning operation, f_i is the load shared by each bunch of this large-tonnage BFRP anchor cable, ϵ_i is the average strain of the BFRP tendons in each bunch of the large-tonnage BFRP anchor cable, and E is the elasticity modulus of the BFRP tendon. S is the cross-sectional area of the BFRP tendon. According to equation (2), based on the measured strain of the BFRP tendon in the tensioning operation, the load-bearing level by the large-tonnage BFRP anchor cable and its difference to the applied tensioning force is achieved (Figure 9).

In the single bunch tensioning stage, the load-bearing level of the large-tonnage BFRP anchor cable is always lower than the applied tensioning force. For instance, as the applied tensioning force is $0.55f_{ptk-1}$ (i.e., 1282.05 kN), the load-bearing level of the large-tonnage BFRP anchor cable is 1189.40 kN. In the tensioning operation, with the increase of the tensioning force, the difference between the load-bearing level and the applied tensioning force presents a convex curve trend. It suggests that, with the increase of



FIGURE 3: The failure mode of the “BFRP-connector-strand.” (a) Steel strand pulled out from the steel connector; (b) BFRP tendon rupture.

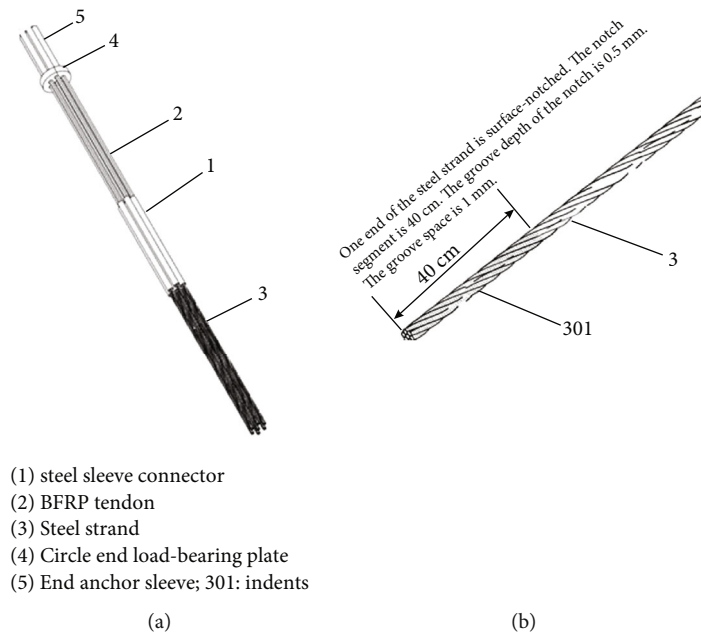


FIGURE 4: The developed large-tonnage pressure-type BFRP cable anchor: (a) the illustration of this developed BFRP cable anchor and (b) the end structure of the steel strand inside the steel sleeve connector.

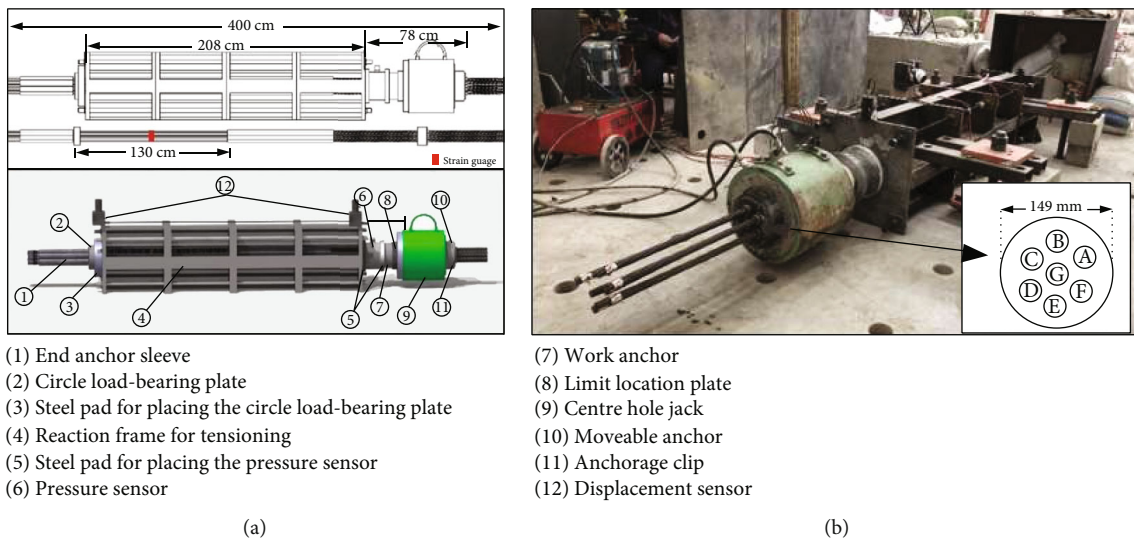


FIGURE 5: The tensile strength test of this BFRP cable anchor: (a) the schematic of the tensioning operation and (b) the indoor tensioning operation where seven bunches of the “BFRP-connector-strand” were numbered with A, B, C, D, E, F, and G.

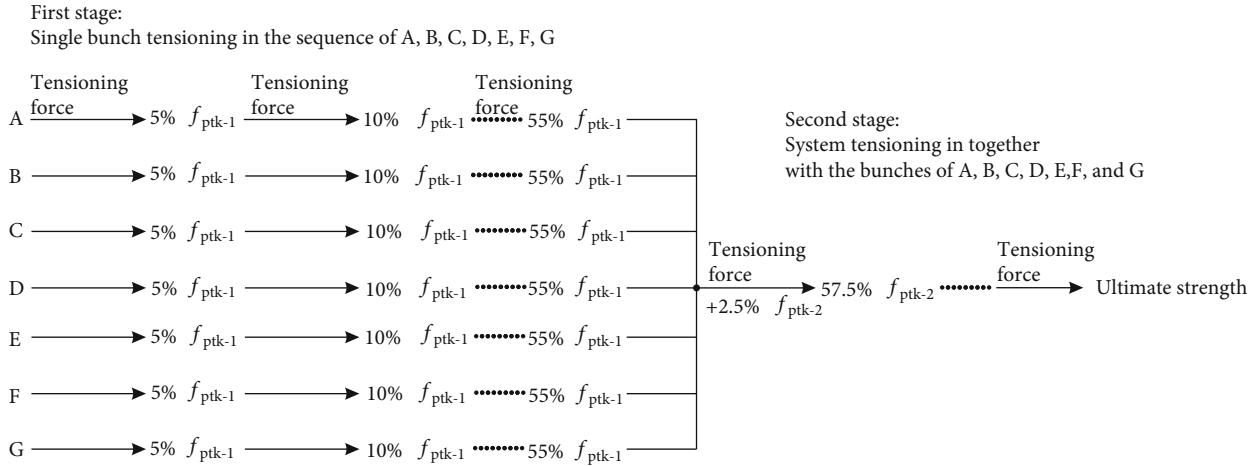


FIGURE 6: The tensioning procedure for the ultimate strength test of this developed large-tonnage BFRP cable anchor.

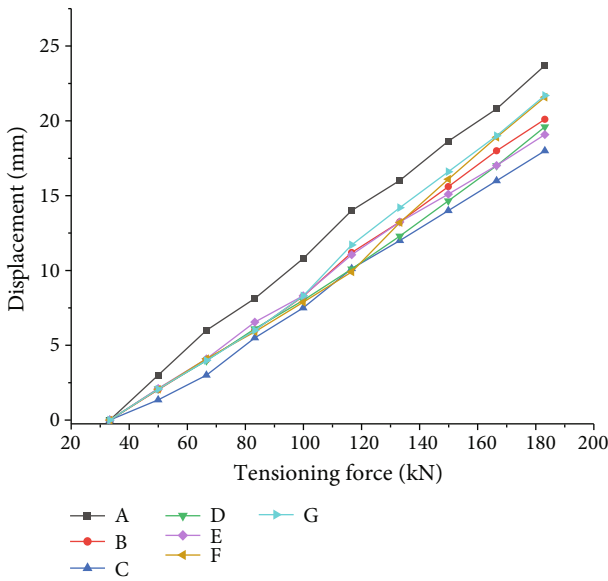


FIGURE 7: The relationship between the elongation and the tensioning force in the stage of single bunch tensioning.

the tensioning force, the stress relaxing effect due to the gap between the interval reaction frame presents a trend of first increase and then decrease. Besides, with the increased tensioning force, the friction resistance among the tensioned BFRP bunches decreases, and then, more prestresses were shared by the BFRP tendons.

3.2. The Mechanical Performance of the Developed BFRP Anchor Cable during the Stage of Systemic Tensioning. Figure 10 shows the relationship between the elongation value and the tensioning force for this large-tonnage BFRP anchor cable in the systemic tensioning. It shows that, with the increase of the tensioning force, there is a linear relationship between the elongation value and the applied tensioning force. As the tensioning force reaches the maximum value of 2023.79 kN (i.e., $0.87f_{ptk-2}$), the system failure of this large-tonnage BFRP anchor cable occurs when the elon-

gation value of this large-tonnage BFRP anchor cable is 23.50 mm (Figure 10(a)). Then, the total elongation value of this large-tonnage BFRP anchor cable can be achieved by adding the value at the process of single bunch tensioning, which is 44.04 mm (Figure 10(b)).

Figure 11 shows the relationship between the strain and the applied tensioning force for this large-tonnage BFRP anchor cable in the process of system tensioning. It should be noted that in the process of system tensioning, with the increase of tensioning force, due to the surface fiber fracture of the BFRP tendons of A-J-3, B-J-1, F-J-3, and G-J-1, the strain collections for these BFRP tendons stop at the strain of 1.41%, 1.54%, 1.47%, and 1.50%. As the tensioning force reaches the ultimate strength of this BFRP anchor cable, the maximum and minimum strains for the BFRP tendons are the B-3 and F-1 BFRP tendon, which are 1.76% and 1.51%, respectively. Besides, the results show that in the process of system tension, there is also a difference in the strain for each BFRP tendon. However, in the system tensioning, each bunch of “BFRP-connector-strand” of this large-tonnage BFRP anchor cable is straightened and tensioned simultaneously. The primary factors for this situation will not be the stress relaxation effect due to the multiple gap compression among the interval reaction frame and not the interval friction resistance of the BFRP tendons. Herein, the possible explanation is that, in the production process of this large-tonnage BFRP anchor cable, the error in the length of the BFRP tendon and the steel strand is inevitably caused by manual operation, such as the cutting operation of the BFRP tendons and the steel strands, and the connecting process of the BFRP tendons and the steel strands in the steel sleeve. Even if it is a tiny difference in the length, it will cause a significant difference in the load-bearing level and strain for each bunch of the “BFRP-connector-strand.” And the shorter the “BFRP-connector-strand” is, the larger the tensioning force is shared and the larger the strain is made in the process of tensioning operation.

Figure 12 shows the tensioning process of this large-tonnage BFRP anchor cable. During the process of system tensioning, as the applied tensioning force reaches the

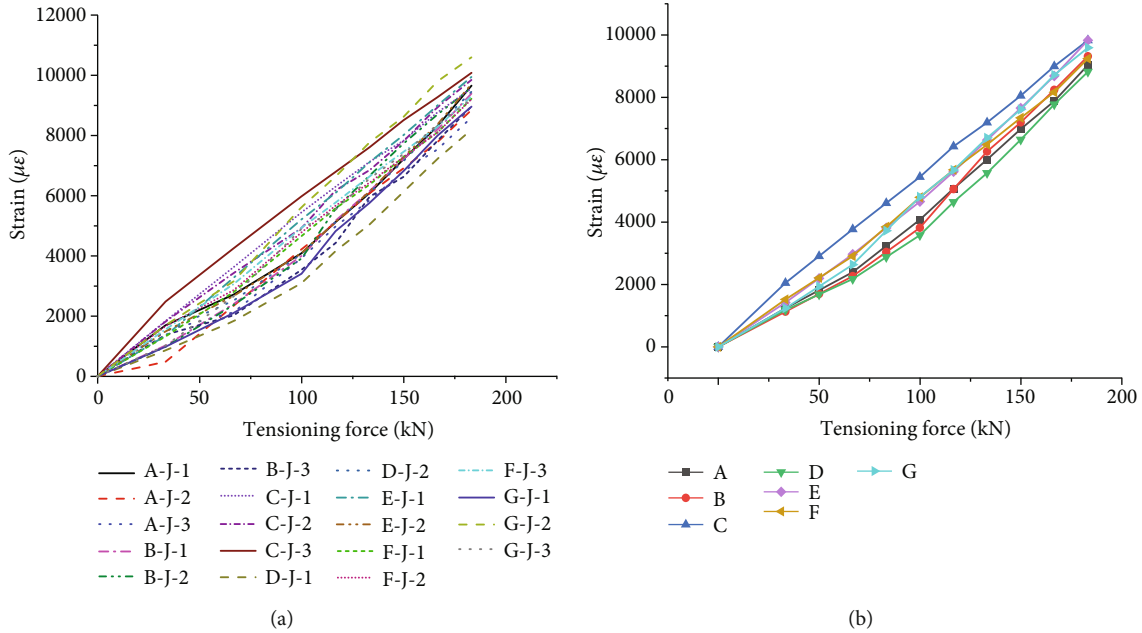


FIGURE 8: The relationship between the strain and the tensoning force: (a) all the BFRP tendons and (b) average for each of the seven bunches.

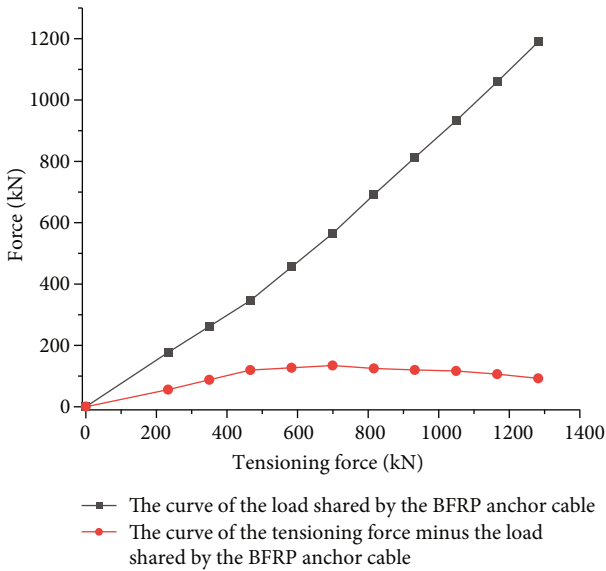


FIGURE 9: The load-bearing level by the large-tonnage BFRP anchor cable in the process of tensoning operation.

ultimate strength of 2023.79 kN (i.e., 202.38 tonnages), this large-tonnage BFRP anchor cable is overburdened and broken (Figure 12(a)). Due to the failure of the “BFRP-connector-strand,” the load-bearing capacity of this BFRP anchor cable decreases suddenly. The dynamic failure process of the “BFRP-connector-strand” was present (Figure 12(b)). It shows that the failure modes of the “BFRP-connector-strand” include three types: the steel strand failure, the middle connector failure, and the BFRP tendons failure. Figure 13 shows the pictures of these failures.

For this BFRP anchor cable, as the applied tensoning force reaches its ultimate strength, first, the steel strand rupture happens for the *D* and *A* bunches (Figure 13(a)), following the middle connector rupture happens for the *B* bunch (Figure 13(b)). Eventually, the BFRP tendon ruptures happen for the *G*, *C*, *E*, and *F* bunches (Figure 13(c)). According to equation (2), based on the measured strain of the BFRP tendons, the load shared by each bunch of the “BFRP-connector-strand” was estimated for the condition of ultimate strength. In the sequence of *A*, *B*, *C*, *D*, *E*, *F*, and *G*, the estimated load values were 291.99 kN, 292.47 kN, 302.47 kN, 284.22 kN, 302.44 kN, 292.04 kN, and 304.79 kN, respectively. It indicates that, as the tensoning force was applied to this BFRP anchor cable, the *G*, *C*, and *E* bunches share the most considerable load; the following are the *B*, *F*, and *A* bunches, and the last is the *D* bunch. This large-tonnage BFRP anchor cable’s ideal failure mode should be the BFRP tendon’s failure instead of the steel strand or the middle connector. Due to the indenting treatment of the steel strand for the *D* and *A* bunches, the depth of the indent is comparatively large. Though this treatment can make a more significant bonding force between the steel strand and the epoxy resin adhesive, the strength of the steel strand decreases. The increased tensoning force makes the steel strand instead of the BFRP tendon first broken. Once the *D* bunch was broken, the tensoning force was transferred immediately to other bunches. For the *B* bunch, the surface-indented steel strand is off-axis in the middle connector, which creates a stress concentration in the area with less epoxy resin adhesive and is shared by the middle connector [24]. Eventually, this off-axis effect makes the middle connector, instead of the BFRP tendon, to be broken.

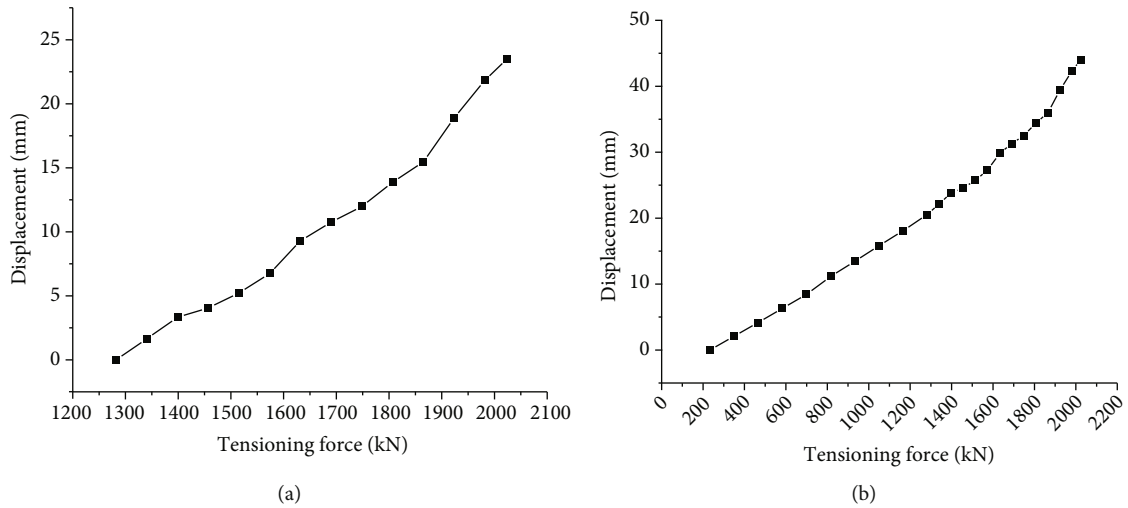


FIGURE 10: The relationship between the elongation and the tensioning force: (a) only the system tensioning and (b) the single bunch tensioning and the system tensioning.

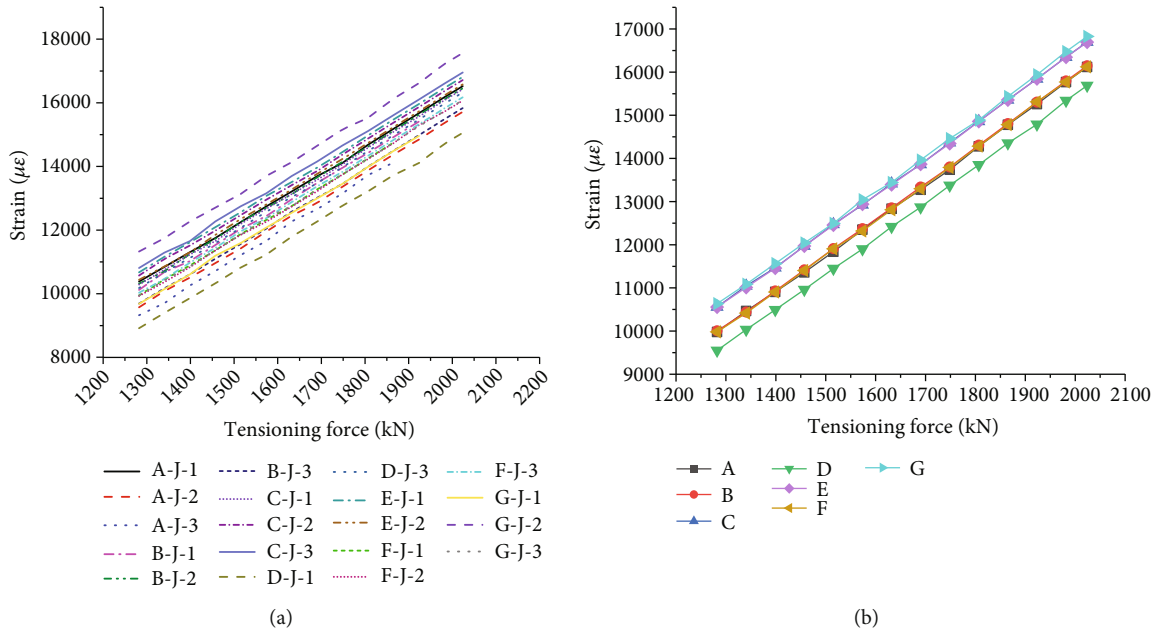


FIGURE 11: The relationship between the strain and the applied tensioning force for this large-tonnage BFRP anchor cable in the stage of the system tensioning: (a) all the BFRP tendons and (b) average of the BFRP tendons for each bunch of the “BFRP-connector-strand.”

3.3. *The Mechanical Mechanism of the Large-Tonnage BFRP Anchor Cable.* For this large-tonnage BFRP anchor cable, during the process of system tensioning, other than the A, B, and D bunches, the C, E, F, and G bunches are broken due to the BFRP tendons rupture at the tensioning force of 302.47 kN, 302.44 kN, 292.04 kN, and 304.79 kN. Those tensioning forces are less than the ultimate strength of the “BFRP-connector-strand.” The reason that caused this issue will be discussed as follows. Before the start of the tensioning operation, there are some gaps between the reaction frames of this tensioning system. As the tensioning force was applied, these gaps are compressed. With the increase of the applied tensioning force, due to the difference in the

length of each bunch “BFRP-connector-strand” of the large-tonnage BFRP anchor cable, the end anchor sleeve is turn up and not vertical to the load-bearing plate (Figure 14). This off-axial phenomenon is general in engineering applications due to the flexural drilling bore or flexural load-bearing plate [24].

Taking one bunch “BFRP-connector-strand” of this large-tonnage BFRP anchor cable as an instance, due to the turnup behavior of the end anchor sleeve, the applied tensioning force will serve as an eccentric force. The coordinate system and physical model were established to analyze the mechanical mechanism of this large-tonnage BFRP anchor cable (Figure 15). For the coordinate system, the x direction

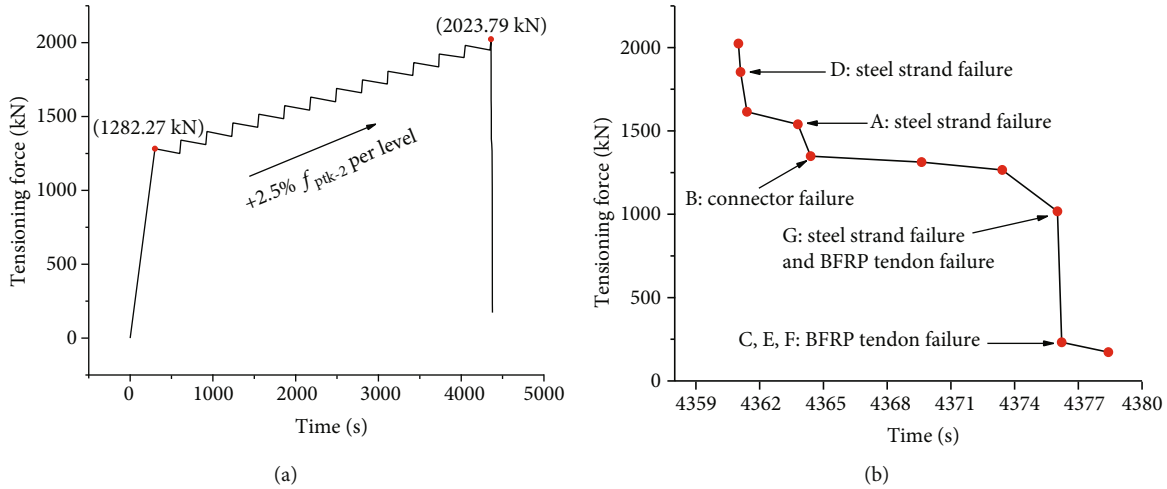


FIGURE 12: The tensioning process of this large-tonnage BFRP anchor cable: (a) the tensioning force with time and (b) the tensioning force with time after the ultimate strength.

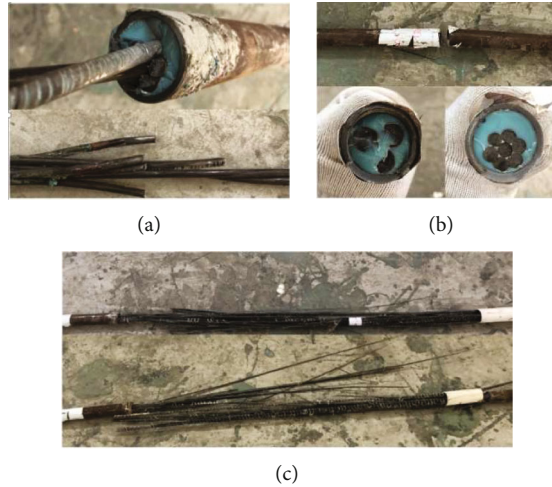


FIGURE 13: The failure mode of this developed large-tonnage BFRP cable anchor: (a) the BFRP rope being broken, (b) the steel strand being broken, and (c) the middle connector being broken.

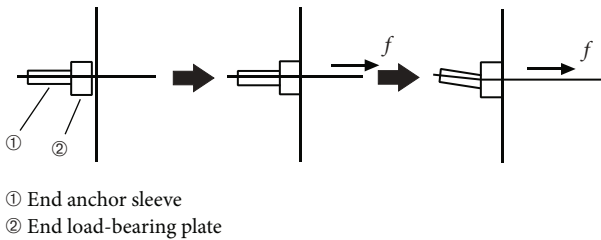


FIGURE 14: The off-axial phenomenon of end anchor sleeve during the tensioning operation.

is along the tensioning direction and passes through the excircle center of the three BFRP tendons in the end anchor sleeve, the y direction is horizontal and mutually perpendicular to the x direction passing through the section centroid of the excircle, and the z direction is vertical and mutually perpendicular to the x direction passing through the section

centroid of the excircle. Then, supposing the eccentric force acts on the P point of the excircle and is a focused force along the x direction (Figure 15(a)).

Based on the above physical model, taking the section centroid of the excircle O as the center point, the turnup behavior of the end anchor sleeve is caused mechanically by three actions: the axial force action along the x direction, the bending moment action at the $x-z$ plane, and the bending moment action at the $x-y$ plane. Of which, the bending moment at the $x-z$ plane and $x-y$ plane can be expressed as follows:

$$\begin{aligned} M_z^o &= f y_f, \\ M_y^o &= f z_f, \end{aligned} \tag{3}$$

where y_f and z_f are the action points of the tensioning force in the y and z directions, respectively.

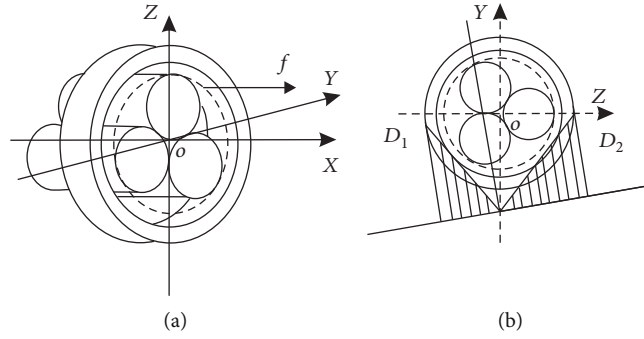


FIGURE 15: The mechanical analysis of the off-axis effect at the contact location of the end anchor sleeve and the end steel load-bearing plate during the tensioning process of this large-tonnage BFRP anchor cable: (a) the mechanical illustration and (b) the loading distribution on the sectional area.

For the system tensioning, any section area of the “BFRP-connector-strand” has the same axial force and bending moment, which can be expressed as follows:

$$\begin{aligned} N &= f, \\ M_y &= M_y^o = fz_f, \\ M_z &= M_z^o = fy_f. \end{aligned} \quad (4)$$

Then, the stress at any point of the section area of the “BFRP-connector-strand” can be expressed as follows [25]:

$$\sigma = \frac{f}{A} + \frac{M_y \cdot z}{I_y} + \frac{M_z \cdot y}{I_z} = \frac{f}{A} \left(1 + \frac{z_f \cdot z}{i_y^2} + \frac{y_f \cdot y}{i_z^2} \right), \quad (5)$$

where A is the effective section area and i_y and i_z are the inertia radius of the section area to the y -axis and z -axis, respectively.

Following, according to the force balance equation for any point at the neutral axis, it can be achieved that

$$1 + \frac{Z_f \cdot Z}{i_y^2} + \frac{y_f \cdot y}{i_z^2} = 0. \quad (6)$$

For the above situation, the neutral axis is a straight line and does not pass the section centroid of the excircle. Then, the y intercept and z intercept of the neutral axis in the established coordinate system can be achieved as follows:

$$\begin{aligned} a_y &= -\frac{i_z^2}{y_f}, \\ a_z &= -\frac{i_y^2}{z_f}. \end{aligned} \quad (7)$$

Then, on the y - z plane, by making a normal line of the neutral axis passing through the point $(0, -(i_z^2/y_f))$, the load distribution around the section area of the end anchor sleeve can be achieved (Figure 15(b)). It shows that, as the end anchor sleeve is off axis, the D_1 and D_2 points in the section

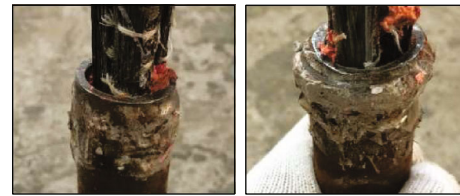


FIGURE 16: The plastic deformation of the end steel anchor sleeve.

area will have the maximum load. Taking the D_2 , the point where the y coordinate is zero as the instance, according to equation (5), the positive stress acting on this point can be expressed as follows:

$$\sigma_D = \frac{f}{A} + \frac{f \cdot (s/d) \cdot (d/2)}{\pi d^4/64} = \frac{f}{A} \left(1 + \frac{4s}{d} \right), \quad (8)$$

where s is the excircle diameter of the end anchor sleeve, 38.00 mm; d is the excircle diameter of the three BFRP tendons inside the end anchor sleeve, 27.15 mm; f is the applied tensioning force; A is the section area of each bunch “BFRP-connector-strand” of this large-tonnage BFRP anchor cable; and f/A means the positive stress under the condition of no off-axis effect, which can be expressed by σ_N . According to equation (8), it can be achieved that $\sigma_D = 6.60 \sigma_N$. As taking no consideration of the end steel sleeve (i.e., $s = d$), it can be achieved that $\sigma_D = 5.00 \sigma_N$. The result shows that, under the condition of the end off-axis effect, as the tensioning force translates to the eccentric loading and serves as a focused force acting on the end BFRP ropes, the positive stress shared by the BFRP ropes will be 5.0 to 6.6 times than that of the normal situation. It means that under the end off-axis effect, the load-bearing capacity of the BFRP anchor cable will be only 15.15% to 20.00% of its ultimate strength. In fact, during the tensioning operation, the shared loading of the C, E, F, and G bunches of the large-tonnage BFRP anchor cable reaches 87.70% to 91.50% of its ultimate strength. It was because, during the BFRP anchor cable tensioning process, both the epoxy resin adhesive and the end steel anchor sleeve have a plastic deformation (Figure 16), which weakens the end off-axis effect. Besides, the tensioning force should be acting at one area of the end steel anchor

sleeve instead of serving as a focused force acting at one point of the end steel anchor sleeve.

4. Conclusions

Basalt fiber-reinforced plastics (BFRP) are a new compound material. Herein, an innovative large-tonnage anchor cable was made with BFRP and its mechanical properties were discussed. The primary conclusions were listed as follows:

This large-tonnage pressure-type prestressed BFRP anchor cable has seven bunch structures of the “BFRP-connector-strand.” In each bunch of the “BFRP-connector-strand,” three BFRP tendons and a steel strand were butting connected inside a steel sleeve connector by the epoxy resin adhesive. During the tensioning operation, the system failure of this large-tonnage BFRP cable anchor is often caused due to the failure of the “BFRP-connector-strand” structure. The failure modes can be classified into steel strand rupture, middle connector rupture, and the BFRP tendon rupture.

The ultimate strength of this BFRP cable anchor can reach 202.38 tonnages. At the ultimate tensioning force condition, the strain of BFRP tendons for this large-tonnage BFRP anchor cable ranges from 1.51% to 1.76%. In the tensioning operation, there is a linear growth relationship between the applied tensioning force and the strain of this BFRP cable anchor.

Due to the length difference of the BFRP tendons, this large-tonnage BFRP cable anchor presents an end-off-axis effect. It makes the load bearing of the BFRP tendons 5.00~6.60 times larger than that of no end off-axis effect. Nevertheless, due to the plastic deformation of the end steel anchor sleeve in the increasing tensioning force, the influence of the end off-axis effect decreases. The load-bearing capacity of this large-tonnage BFRP cable anchor reaches 87.70~91.50% of its theoretical value.

Data Availability

The data used to support the findings of this study are included within the article.

Conflicts of Interest

The authors declare that there is no interest conflict for publishing this study.

Acknowledgments

This study has been sponsored financially by the Natural Science Foundation of Henan Province (Project no. 222300420242), the Science and Technology Development Project of Luoyang (Project no. 2101025A), the Heluo Young Talent Lifting Project of Society and Technology Association of Luoyang (Project no. 2022HLTJ06), the Science and Technology Innovation Leading Talent Project of Zhongyuan (Project no. 214200510030), and the Key Research and Development Project of Henan Province (Project no. 221111321500).

References

- [1] S. Robert, T. Michal, and K. Stanislav, “Analysis of wind-induced vibrations of an anchor cable using a simplified fluid-structure interaction method,” *Applied Mathematics and Computation*, vol. 267, pp. 223–236, 2015.
- [2] Y. Xue, J. Liu, P. G. Ranjith, F. Gao, Z. Zhang, and S. Wang, “Experimental investigation of mechanical properties, impact tendency, and brittleness characteristics of coal mass under different gas adsorption pressures,” *Geomechanics and Geophysics for Geo-Energy and Geo-Resources*, vol. 8, no. 5, article 131, 2022.
- [3] D. Zheng, F. Z. Liu, N. P. Ju, J. D. Frost, and R. Q. Huang, “Cyclic load testing of pre-stressed rock anchors for slope stabilization,” *Journal of Mountain Science*, vol. 13, no. 1, pp. 126–136, 2016.
- [4] J. Y. Xue, J. Liu, P. G. Ranjith, F. Gao, H. Xie, and J. Wang, “Changes in microstructure and mechanical properties of low-permeability coal induced by pulsating nitrogen fatigue fracturing tests,” *Rock Mechanics and Rock Engineering*, no. - article 3031, 2022.
- [5] N. Elmessalami, F. Abed, and R. A. Ei, “Response of concrete columns reinforced with longitudinal and transverse BFRP bars under concentric and eccentric loading,” *Composite Structures*, vol. 255, article 113057, pp. 1–12, 2021.
- [6] S. Divi, D. Chandra, and J. Daemen, “Corrosion susceptibility of potential rock bolts in aerated multi-ionic simulated concentrated water,” *Tunnelling and Underground Space Technology*, vol. 26, no. 1, pp. 124–129, 2011.
- [7] M. J. Hutchison, *Corrosion of Post-Tensioning Strands in UngROUTED DUCTS-UNSTRESSED CONDITION*, USA: Graduate Theses and Dissertations, USA FIA: University of South Florida, 2013.
- [8] L. I. Zheng, W. A. Bo, H. E. Chuan, L. Fu-hai, Z. Pei, and S. Yang, “Experimental study of corrosion resistance of multiple anticorrosive bolts,” *Rock and Soil Mechanics*, vol. 36, no. 4, pp. 1071–1077, 2015.
- [9] S. Permeah, K. K. K. Vigneshwaran, M. Echeverria, K. Lau, and I. Lasa, “Corrosion of post-tensioned tendons with deficient grout, part 2: segregated grout with elevated sulfate content,” *Corrosion*, vol. 74, no. 4, pp. 457–467, 2018.
- [10] C. L. Alexander and M. E. Orazem, “Indirect impedance for corrosion detection of external post-tensioned tendons: 2. multiple steel strands,” *Corrosion Science*, vol. 164, no. 164, article 108330, 2020.
- [11] V. Lopresto, C. Leone, and I. D. Iorio, “Mechanical characterisation of basalt fibre reinforced plastic,” *Composites Part B: Engineering*, vol. 42, no. 4, pp. 717–723, 2011.
- [12] P. Larrinaga, C. Chastre, H. C. Biscaia, and J. T. San-Jose, “Experimental and numerical modeling of basalt textile reinforced mortar behavior under uniaxial tensile stress,” *Materials and Design*, vol. 55, pp. 66–74, 2014.
- [13] V. J. John and B. Dharmar, “Influence of basalt fibers in the mechanical behavior of concrete—a review,” *Structural Concrete*, vol. 22, pp. 491–502, 2021.
- [14] X. Wang, P. C. Xu, Z. S. Wu, and J. Z. Shi, “A novel anchor method for multi-tendon FRP cable: concept and FE study,” *Composite Structures*, vol. 120, pp. 552–564, 2015.
- [15] J. Feng, Y. Wang, Y. F. Zhang, L. Huang, C. J. He, and W. U. Hong-gang, “Experimental comparison of anchorage performance between basalt fiber and steel bars,” *Rock and Soil Mechanics*, vol. 40, no. 11, pp. 4185–4193, 2019.

- [16] W. He, X. Wang, and Z. Wu, "Flexural behavior of RC beams strengthened with prestressed and non- prestressed BFRP grids," *Composite Structures*, vol. 246, no. 246, article 112381, 2020.
- [17] H. M. Diab and A. M. Sayed, "An anchorage technique for shear strengthening of RC T-beams using NSM-BFRP bars and BFRP sheet," *International Journal of Concrete Structures and Materials*, vol. 14, no. 1, pp. 49–65, 2020.
- [18] T. W. Lai, H. Lei, Z. X. Wu, and H. G. Wu, "Shaking table test study on basalt fiber reinforced plastics in high slope protection," *Rock and Soil Mechanics*, vol. 42, no. 2, pp. 390–400, 2021.
- [19] V. Dhand, G. Mittal, K. Y. Rhee, and D. Hui, "A short review on basalt fiber reinforced polymer composites," *Composites Part B: Engineering*, vol. 73, pp. 166–180, 2015.
- [20] X. L. Wu, Y. Q. Wei, Z. W. Dai et al., "Study of mechanical properties and failure modes of basalt fiber reinforced polymer bonded anchor cable," *Journal of Henan University of Science and Technology (Natural Science)*, vol. 42, no. 5, pp. 51–56, 2021.
- [21] Q. X. Fan, P. C. Wei, P. Lin, and J. Geng, "Study on excavating and reinforcement stability on the south slope of the north gate head of the Three Gorges ship lock," *Chinese Journal of Rock Mechanics and Engineering*, vol. 39, no. 1, pp. 2703–2712, 2020.
- [22] L. J. Wang, Y. Zhang, T. Jiang, X. B. Li, A. J. Mao, and W. X. Mao, "Chinese National Standard: steel strand for prestressed concrete," General Administration of Quality Supervision, Inspection and Quarantine of the People's Republic of China, 20 pages, 2015.
- [23] D. B. Feng, X. Chen, X. J. Xu, Y. D. Jiang, L. Zeng, and K. P. Tian, "Chinese National Standard: Anchorage, grip and coupler for prestressing tendons," General Administration of Quality Supervision, Inspection and Quarantine of the People's Republic of China, 32 pages, 2015.
- [24] Y. M. Li, N. J. Ma, and K. Yang, "Experiment research on the FRP bolt under eccentric load," *FRP/Composite*, vol. 4, pp. 86–88, 2009.
- [25] Z. C. Chen, Q. X. Wang, and J. P. Wang, *Mechanics of Materials*, Chin U Min Tech Press, China Xuzhou, 1994.